

NASA TECHNICAL NOTE



NASA TN D-4432

C.1

NASA TN D-4432



LOAN COPY: RETURN TO
AFWL (WLIL-2)
KIRTLAND AFB, N MEX

EXPERIMENTAL PERFORMANCE EVALUATION OF
AN 8.5-INCH- (21.59-CM-) MEAN-DIAMETER
AXIAL-FLOW TURBINE AT REYNOLDS NUMBERS
FROM 18 000 TO 177 000

by William J. Nusbaum and Milton G. Kofskey

Lewis Research Center

Cleveland, Ohio



EXPERIMENTAL PERFORMANCE EVALUATION OF AN 8.5-INCH-
(21.59-CM-) MEAN-DIAMETER AXIAL-FLOW TURBINE AT
REYNOLDS NUMBERS FROM 18 000 TO 177 000

By William J. Nusbaum and Milton G. Kofskey

Lewis Research Center
Cleveland, Ohio

NATIONAL AERONAUTICS AND SPACE ADMINISTRATION

For sale by the Clearinghouse for Federal Scientific and Technical Information
Springfield, Virginia 22151 - CFSTI price \$3.00

EXPERIMENTAL PERFORMANCE EVALUATION OF AN 8.5-INCH-
(21.59-CM-) MEAN-DIAMETER AXIAL-FLOW TURBINE AT
REYNOLDS NUMBERS FROM 18 000 TO 177 000

by William J. Nusbaum and Milton G. Kofskey

Lewis Research Center

SUMMARY

An experimental investigation of an 8.5-inch- (21.59-cm-) mean-diameter, two-stage, axial-flow turbine was conducted to determine the effect of a change in Reynolds number on the performance of a turbine of this type and size. The investigation was conducted with cold argon over a range of inlet pressures from about 1.0 to 9.0 psia (0.68 to 6.2 N/cm² abs) with corresponding Reynolds numbers from 18 000 to 177 000. (Reynolds number, as used herein, is defined as the ratio of the mass flow to the product of viscosity and rotor mean radius, where the viscosity is determined at the turbine-inlet condition.) At each value of turbine-inlet pressure, data were taken at design equivalent speed and various pressure ratios.

Results of the investigation indicated that at design equivalent speed and pressure ratio an increase in Reynolds number resulted in a 5.8 percent increase in mass flow over the range of Reynolds number covered. This variation occurred because of the decreased stator viscous losses and in a manner similar to that predicted from reference fluid meter data. The total efficiency at design equivalent speed and pressure ratio increased from 0.82 to 0.88 with an increase in Reynolds number over the same range. The corresponding static efficiency increased from 0.80 to 0.86. This increase in efficiency was attributed to the associated decrease in viscous losses since the rotor reaction was independent of Reynolds number.

The variation in loss with change in Reynolds number agreed well with a theoretical variation, wherein 0.7 of the loss was attributed to viscous losses and the remaining 0.3 was attributed to other losses which are independent of Reynolds number. This variation is similar to that for two reference radial turbines investigated over a comparable range of Reynolds number.

INTRODUCTION

Turbines designed for Brayton-cycle space power systems are currently being investigated at Lewis. Included in this program is a reference two-shaft system which uses a small high-speed turbine to drive the compressor and a low-speed turbine to power the alternator (ref. 1). The low power output of this type of system (characteristically, 1 to 10 kW) requires that the associated turbines (in particular, the alternator drive turbine) operate at low Reynolds numbers.

Both radial-inflow and axial turbines have been investigated in the past to determine the influence of Reynolds number on efficiency (refs. 2 to 6). Results of these studies indicate a deterioration in performance as Reynolds number is reduced below a certain level. In addition, studies, such as those in reference 7, indicate that the efficiency level of the turbines for this application is important.

As a result of these investigations, it was considered important to determine the effect of Reynolds number on the performance of the alternator drive turbine specifically designed for the aforementioned reference Brayton system. The aerodynamic performance of this 8.5-inch- (21.59-cm-) mean-diameter, two-stage, axial-flow turbine at approximately the design Reynolds number of 49 500 is presented in reference 8. (Reynolds number as used herein is defined as the ratio of the mass flow to the product of viscosity and rotor mean radius, where the viscosity is determined at the turbine-inlet condition.) This report presents the results of the extension of this investigation to encompass Reynolds numbers considerably above and below the design value, obtained by varying the turbine-inlet pressure. Performance tests of the turbine were made with argon as the working fluid at a turbine-inlet temperature of 610°R (339°K) and at five values of inlet pressure ranging from about 1.0 to 9.0 psia (0.68 to 6.2 N/cm^2 abs). At design equivalent speed and pressure ratio, this range of inlet pressure corresponds to a range of Reynolds number from about 18 000 to 177 000. (Results of the tests near the design Reynolds number of 49 500 are presented in ref. 8 and are repeated herein.) At each inlet pressure, data were obtained at design equivalent speed over a range of pressure ratios. The results of the investigation are presented in terms of equivalent mass flow, efficiency, and a loss parameter. Aerodynamic losses in the subject turbine are then compared with those measured in reference radial- and axial-flow turbines.

TURBINE DESCRIPTION

The turbine used in this investigation was the same as that described in reference 8. For convenience, however, design values, velocity diagrams, and some of the more important features of the turbine are repeated herein. Design point values with argon as

the working fluid and also the air-equivalent (U. S. standard sea-level) design values are as follows:

Argon:

Turbine rotative speed, N , rpm	12 000
Specific work, Δh , Btu/lb (J/g)	15.04 (35.010)
Mass flow, w , lb/sec (kg/sec)	0.611 (0.277)
Inlet total temperature T'_1 , $^{\circ}\text{R}$ ($^{\circ}\text{K}$)	1685 (936.11)
Inlet total pressure, p'_1 , psia (N/cm^2 abs)	8.45 (5.826)
Blade-jet speed ratio, ν	0.465
Reynolds number, $\text{Re} = w/\mu r_m$	49 500
Total to total efficiency, η_t	0.850
Total to static efficiency, η_s	0.825
Total- to total-pressure ratio, p'_1/p'_5	1.2469
Total- to static-pressure ratio, p'_1/p_5	1.2542

Air equivalent (U. S. standard sea level):

Rotative speed, $N/\sqrt{\theta_{cr}}$, rpm	7554
Specific work, $\Delta h/\theta_{cr}$, Btu/lb (J/g)	5.96 (13.874)
Mass flow, $\epsilon w\sqrt{\theta_{cr}}/\delta$, lb/sec (kg/sec)	1.537 (0.697)
Torque $\tau\epsilon/\delta$, in.-lb (N-m)	108.12 (12.216)
Total- to total-pressure ratio, $p'_1/p'_{5,eq}$	1.225
Total- to static-pressure ratio, $p'_1/p_{5,eq}$	1.233
Blade-jet speed ratio, ν	0.465

Equivalent pressure ratios were calculated from equivalent specific work in air and with the assumption of no change in efficiency when argon or air is used as the working fluid.

The design velocity diagrams are presented in figure 1. The diagrams indicate a conservative aerodynamic design with a relatively low level of velocity through both stages and a large amount of reaction.

The stator design is conventional; 44 blades for the first stage and 40 blades for the second stage give respective values of solidity at the mean diameters of 1.57 and 1.56. The rotor design incorporated 36 blades in each of the two stages with tip diameters of 9.7 and 9.8 inches (24.64 and 24.89 cm) for the first and second stages, respectively. The resulting values of solidity at the mean diameter were 1.3 and 1.4. The rotor assembly is shown in figure 2. Two characteristic features of both rotors are the large amount of blade twist and the comparatively low value of solidity at the tip, both of which contribute to a short guided channel in the region of the blade tip.

Figure 3 presents a cross-sectional view of the turbine showing the arrangement of

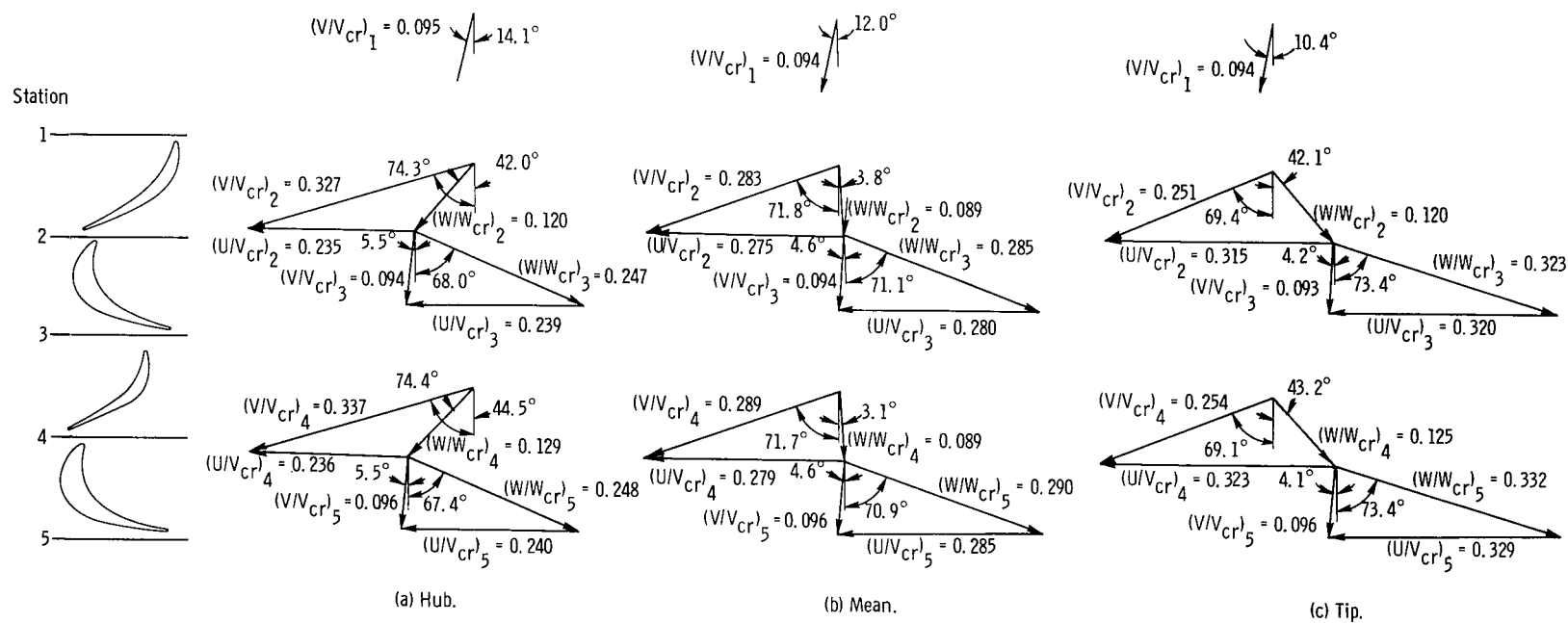
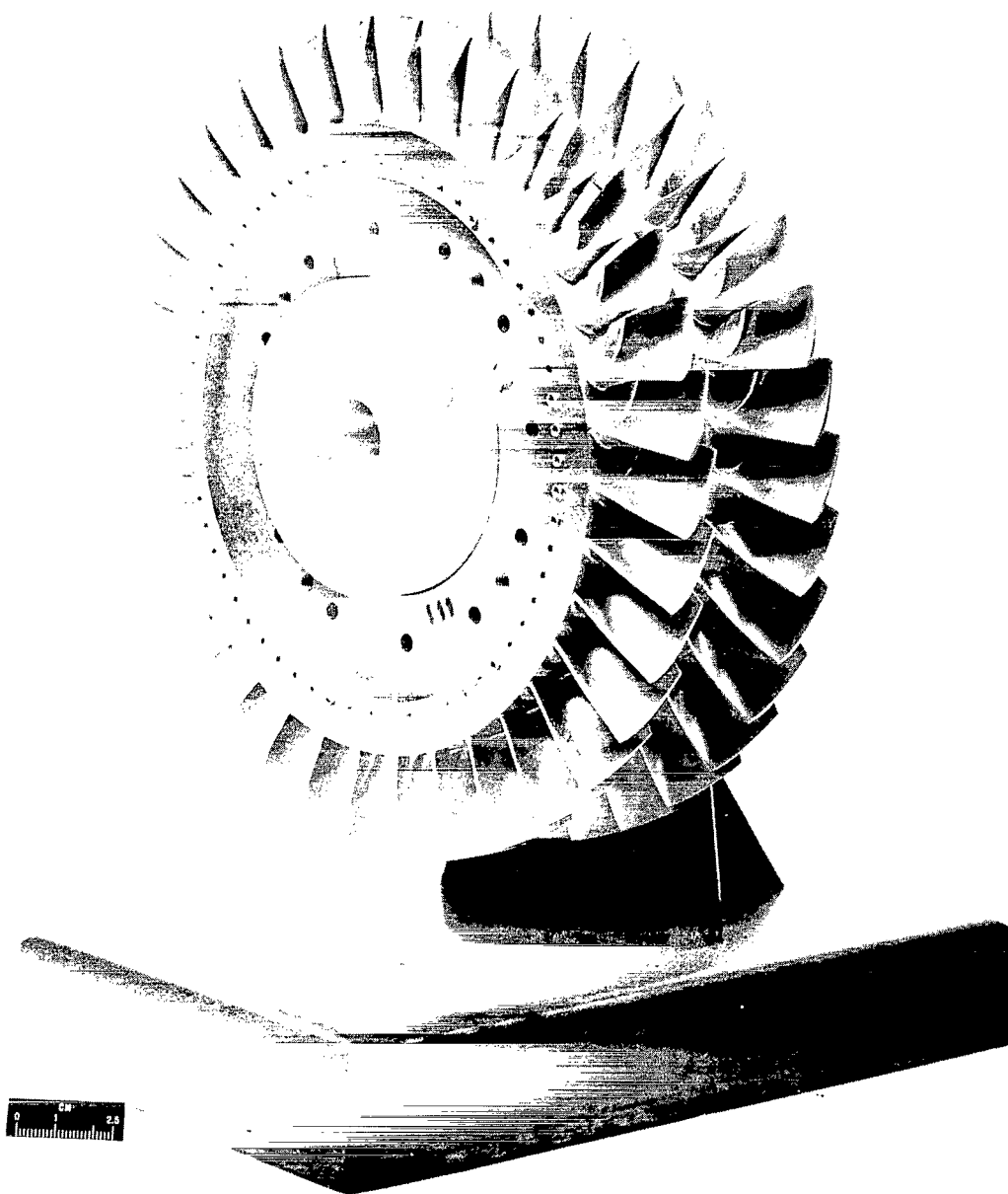
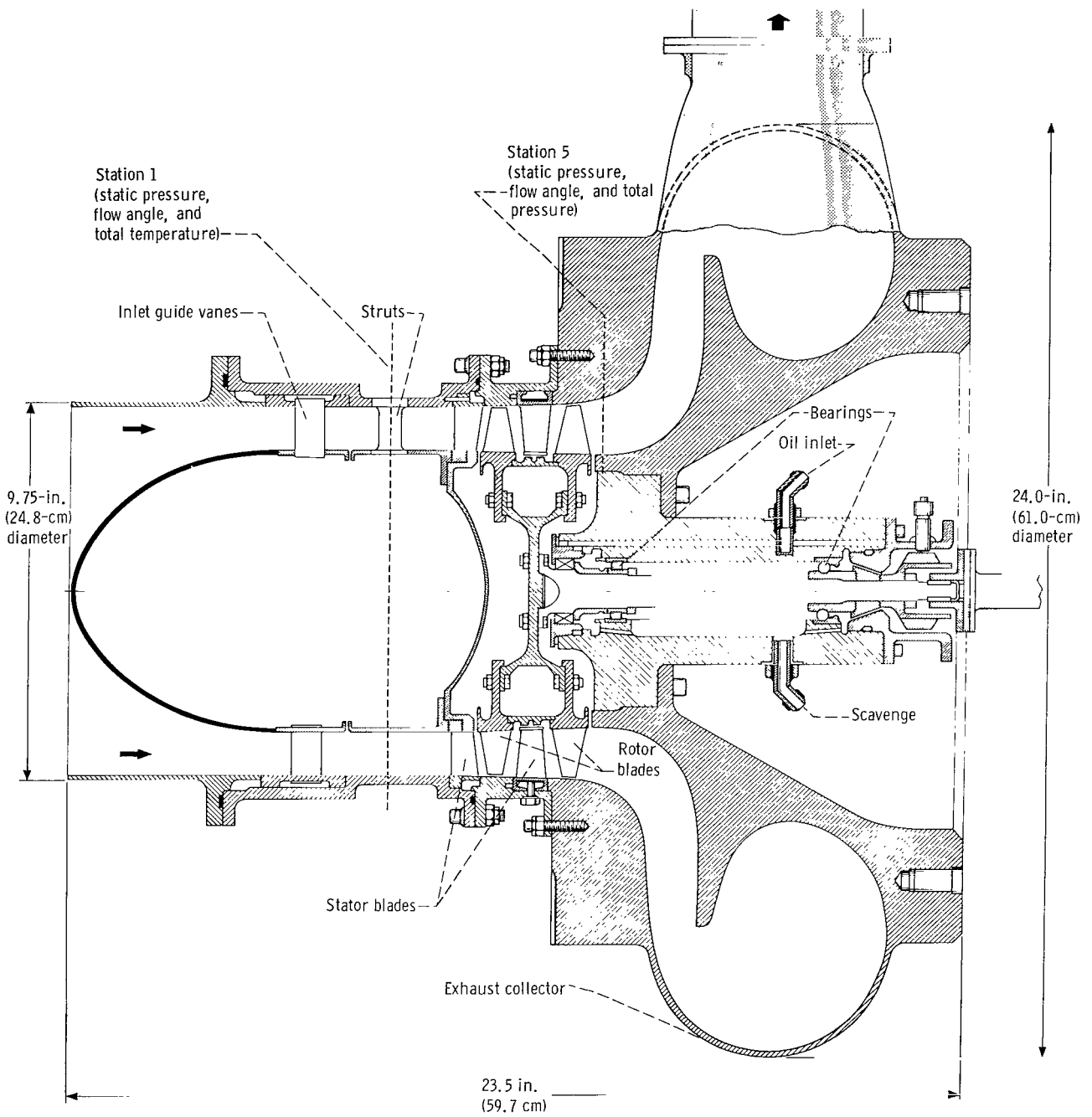


Figure 1. - Design velocity diagrams.



C-66-3770

Figure 2. - Two-stage turbine rotor assembly.



CD-9272

Figure 3. - Cross section of turbine.

the blading and the gas flow passages. These passages have a sharp, radially outward turn immediately downstream of the second-stage rotor. However, the sudden change in flow direction caused little loss in total pressure because of the low level of gas velocity. This result is verified by the results presented in reference 8.

APPARATUS, INSTRUMENTATION, AND TEST PROCEDURE

The apparatus consisted of the turbine, an airbrake dynamometer to absorb and measure the power output of the turbine, and an inlet and exhaust piping system with flow controls. A schematic drawing of the experimental equipment is shown in figure 4.

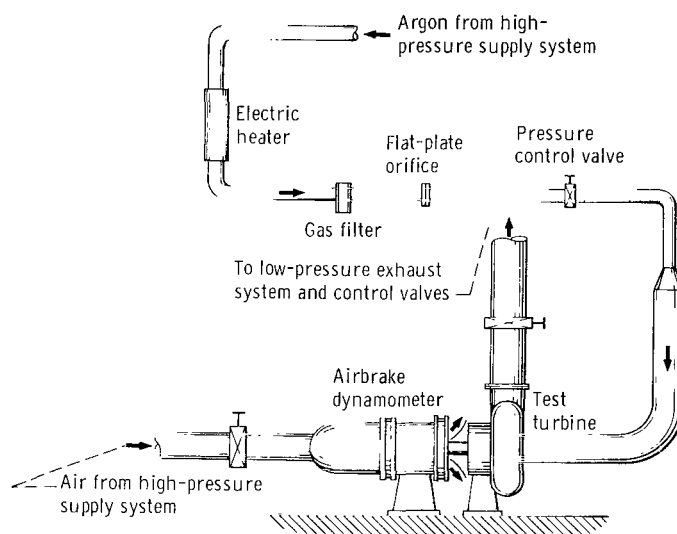


Figure 4. - Schematic of test equipment.

CD-9274

Pressurized argon was used as the driving fluid for the turbine. The argon was piped into the turbine through an electric heater, a filter, a mass-flow measuring station that consisted of a calibrated flat-plate orifice, and a remotely controlled pressure-regulating valve. The gas, after expanding through the turbine, was passed through a remotely controlled exhaust valve and into the laboratory low-pressure exhaust system. With a fixed inlet pressure, the remotely operated valve in the exhaust line was used to obtain the desired pressure ratio across the turbine.

The airbrake dynamometer, which was cradle mounted to measure torque, absorbed and measured the power output of the turbine and, at the same time, controlled the speed. The force on the torque arm was measured with a commercial strain-gage load cell.

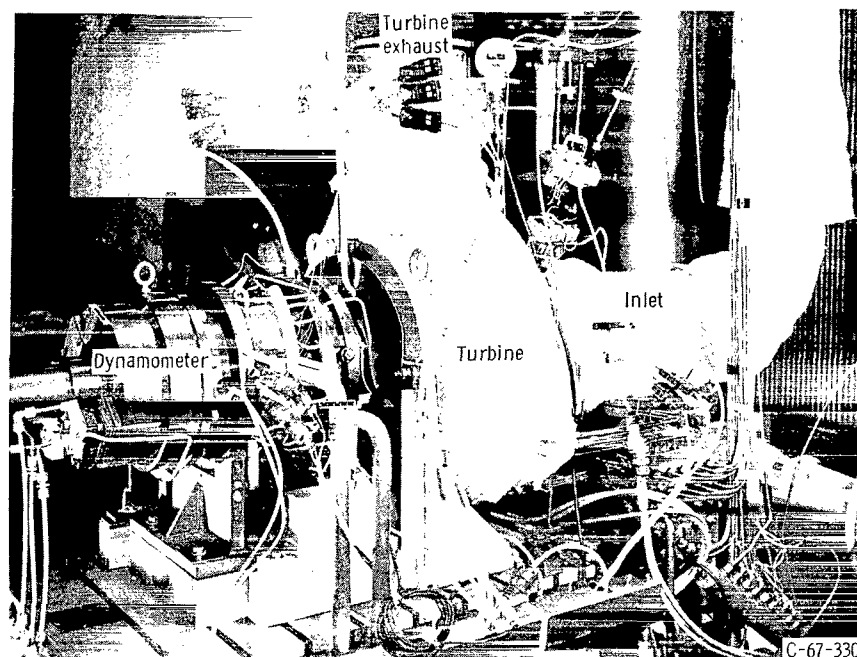


Figure 5. - Experimental turbine test setup.

The rotational speed was measured with an electronic counter in conjunction with a magnetic pickup and a shaft-mounted gear. The turbine test facility is shown in figure 5.

The measuring stations are shown in figure 3. A detailed description of the instrumentation is given in reference 8. Briefly, instrumentation was installed at the turbine inlet (station 1) and immediately downstream of the second-stage-rotor trailing edge (station 5) to determine both the static and total efficiencies.

The absolute values of the pressures below about 3.5 psi (2.4 N/cm^2) were measured by the use of manometer tubes containing a fluid of low specific gravity (1.04) and evacuated to a pressure of about 10 microns of mercury (0.00013 N/cm^2) on the reference side of the tube. Higher pressures were measured by pressure transducers and together with all other data were recorded by an automatic digital potentiometer and processed through an electronic digital computer.

Performance data were taken at an inlet total temperature of about 610° R (339° K) and at eight values of inlet pressure ranging from about 1.0 to 9.0 psia (0.68 to 6.2 N/cm^2 abs). This variation in inlet pressure resulted in a range of Reynolds number from 18 000 to 177 000 at design equivalent speed and pressure ratio. (Reynolds number as used herein is defined as $Re = w/\mu r_m$, where the viscosity is determined at the turbine-inlet condition.) The values of inlet total pressure and temperature along with corresponding Reynolds numbers at design equivalent speed and pressure ratio are shown in table I. At each inlet pressure, data were obtained at design equivalent speed and over

TABLE I. - INLET CONDITIONS CORRESPONDING
TO REYNOLDS NUMBERS INVESTIGATED

[Inlet total temperature, 610° R (339° K).]

Reynolds number, Re	Inlet total pressure	
	psia	N/cm ² abs
18 000	0.98	0.68
28 000	1.49	1.03
^a 47 400	^a 2.50	1.72
62 000	3.19	2.20
97 000	4.95	3.41
137 000	7.00	4.83
159 000	8.02	5.53
177 000	9.01	6.21

^aObtained from ref. 8.

a range of total- to static-pressure ratio. The range of pressure ratios differed for the various inlet pressures because of limitations of the airbrake dynamometer. However, all pressure ratios were within the range of 1.08 to 1.65.

Friction torque of the bearings and seals was measured by the method described in reference 8. A friction torque value of approximately 1.0 inch-pound (0.113 N-m) was obtained at design equivalent rotative speed. This value corresponds to about 16.2 and 1.3 percent of the turbine work at turbine-inlet absolute pressures of 1.0 and 9.0 psi (0.68 and 6.2 N/cm²), respectively. The friction torque was added to the shaft torque to obtain the turbine work.

Turbine efficiency was computed as the ratio of actual turbine work to ideal turbine work. The turbine was rated on the basis of both total and static efficiency. Turbine-inlet and turbine-outlet total pressures were calculated from values of mass flow, static pressure, total temperature, and flow angle.

RESULTS AND DISCUSSION

The subject turbine was investigated over a range of inlet pressures from approximately 1.0 to 9.0 psia (0.68 to 6.2 N/cm² abs) at design equivalent speed and at various pressure ratios. For operation at design equivalent pressure ratio, this range of inlet pressures corresponds to a range of Reynolds number from about 18 000 to 177 000. Performance results near design Reynolds number of 49 500 were obtained from reference 8. Results are presented in two sections. First, the performance of the subject

axial-flow turbine is discussed. Then the performance of the subject turbine is compared with that of several other turbines.

Turbine Performance

Figure 6 shows the variation of equivalent mass flow $\epsilon w \sqrt{\theta_{cr}} / \delta$ with equivalent turbine exit-static- to inlet-total-pressure ratio, for operation at design equivalent speed

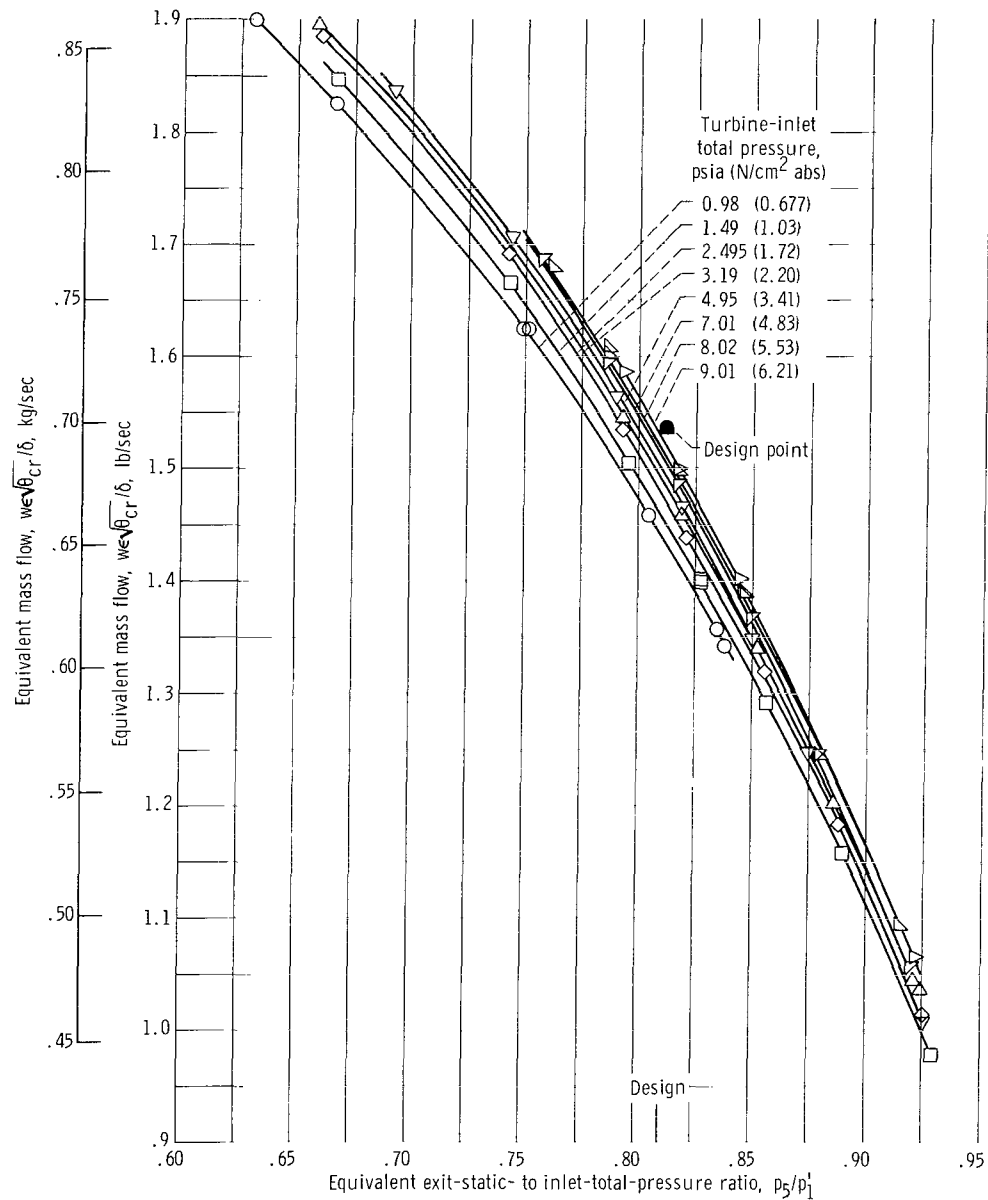


Figure 6. - Variation of mass flow with pressure ratio and turbine-inlet total pressure at design equivalent speed.

and at eight values of turbine-inlet pressure. For any given inlet pressure, the variation of mass flow with pressure ratio is typical of subsonic turbines. At any pressure ratio, there is a small increase in equivalent mass flow with an increase in turbine-inlet pressure. In addition, design equivalent mass flow of 1.537 pounds per second (0.697 kg/sec) was not obtained over the range of inlet pressures investigated. As stated in reference 8, the deficiency in mass flow was attributed to the flow areas in the blade rows being from 3 to 8 percent smaller than design.

The variation in equivalent mass flow with Reynolds number at design equivalent pressure ratio is shown in figure 7, which is a cross plot of figure 6. As shown in figure 7, there was an approximate 5.8 percent increase in equivalent mass flow when Reynolds number was increased from 18 000 to 177 000.

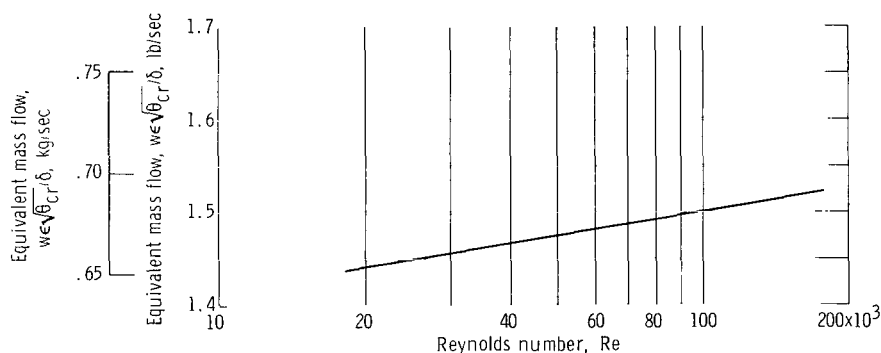


Figure 7. - Variation of mass flow with Reynolds number at design equivalent speed and pressure ratio.

The reaction across the first-stage stator was determined from the static-pressure measurements in order to determine the principal cause for this mass-flow variation. Within experimental accuracy, this reaction was unchanged over the entire range of Reynolds number covered, which indicates that the flow variation was attributable to decreased viscous losses within the stator. This flow variation was then compared with that predicted by using long-radius flow nozzle criteria, as presented in reference 9. These calculations indicated a coefficient of discharge varying from approximately 0.92 to 0.97 over the Reynolds number range covered, which agrees closely with that obtained in the subject investigation.

The variations of total and static efficiencies with blade-jet speed ratio for the eight values of turbine-inlet total pressure are shown in figure 8. As shown in the figure, the range of blade-jet speed ratios was limited when operating at either the smaller or larger values of turbine-inlet pressure. As mentioned in APPARATUS, INSTRUMENTATION, AND TEST PROCEDURE, these restrictions were the result of limitations of the airbrake dynamometer. The total efficiency curves show similar trends for all inlet

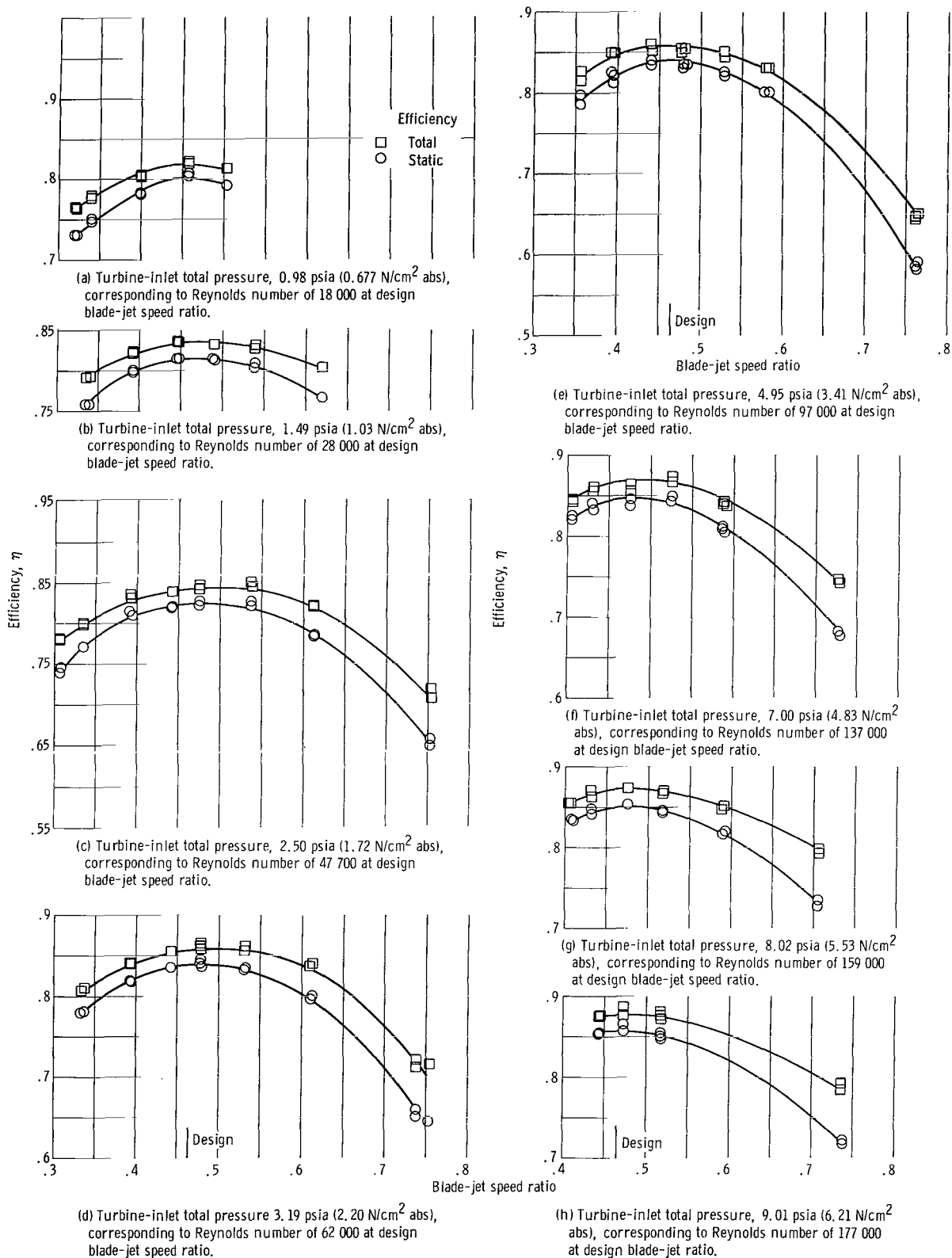


Figure 8. - Performance characteristics over range of turbine-inlet pressures.

pressures. These curves indicate a maximum value of efficiency at or near the design value of blade-jet speed ratio. The static-efficiency curves show trends similar to those of the total-efficiency curves with a difference between the two curves of only about 2 percentage points near design blade-jet speed ratio. This small difference results from the low levels of exit kinetic energy.

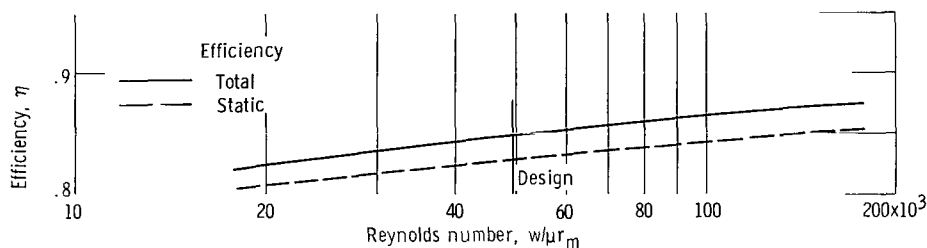


Figure 9. - Effect of Reynolds number on turbine efficiency at design equivalent speed and pressure ratio.

Figure 9 presents the variation of total and static efficiencies with Reynolds number at design equivalent speed and pressure ratio. The trend of increasing efficiency with increasing Reynolds number is quite apparent from both curves. For the range of Reynolds number covered in the investigation, there was an increase in total efficiency from about 0.82 to 0.88 and a corresponding increase in static efficiency from about 0.80 to 0.86.

It was found possible in reference 6 for turbine performance to deteriorate very rapidly at Reynolds numbers below 60 000 and for the turbine to operate at any one of several efficiencies at any given blade-jet speed ratio. This latter phenomenon was attributed to varying amounts of negative reaction across the rotor, with the resultant varying degrees of flow separation at the rotor exit. However, such effects were not encountered in the subject investigation even though correspondingly low Reynolds numbers were covered. We concluded that the relatively high blade reactions prevented the occurrence of these unusual effects in the subject turbine investigation.

Performance Comparison with Reference Turbines

The subject turbine is compared with four other turbines, two (refs. 2 and 3) of the radial-inflow type and two (refs. 4 and 5) of the axial-flow type. Performance data are presented for the turbines at their respective design equivalent speeds and pressure ratios and over a range of Reynolds number comparable to that of the subject investigation.

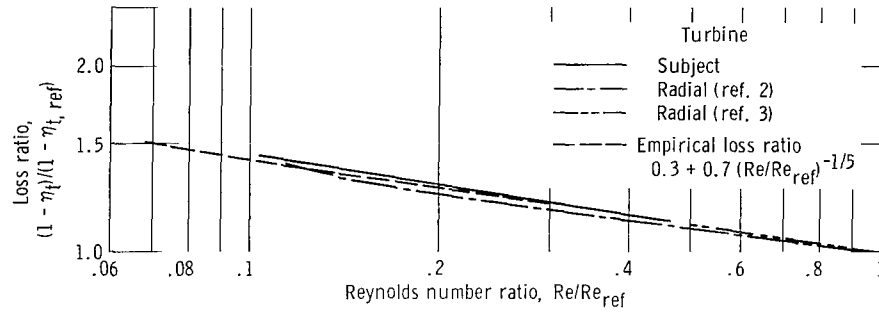


Figure 10. - Comparison of loss ratios as function of Reynolds number at design equivalent speed and pressure ratio.

Comparison with radial-inflow turbines. - In figure 10, the subject turbine is compared with the two radial-inflow turbines, all of which are included in the investigations of the 10-kilowatt Brayton-cycle system and components. Performance is expressed in terms of a loss ratio $(1 - \eta_t)/(1 - \eta_{t, \text{ref}})$ where $1 - \eta_{t, \text{ref}}$ was evaluated at a reference Reynolds number of 177 000. The figure shows the variation of this loss ratio with the Reynolds number ratio Re/Re_{ref} and indicates good agreement between the subject turbine and either of the reference turbines.

As shown in reference 10, the variation between loss ratio and Reynolds number can be expressed by an equation of the form

$$\frac{1 - \eta_t}{1 - \eta_{t, \text{ref}}} = A + B \left(\frac{Re}{Re_{\text{ref}}} \right)^{-1/5}$$

where viscous losses due to skin friction are associated with the Reynolds number term, and where the values of the constants A and B depend on the relative values of viscous losses and design factors, such as rotor-blade tip clearance, blade surface diffusion, and loading. Figure 10 shows a theoretical curve which expresses this relation with values assigned to the constants as follows: $A = 0.3$ and $B = 0.7$. Excellent agreement is evident between the theoretical curve and the experimental curves of the subject and reference turbines. The experimental curves of the subject turbine and of the radial turbine of reference 3 coincide.

Comparison with reference axial-flow turbines. - In addition to the comparison just made, it is of interest to compare the trends of efficiency loss with Reynolds number for the subject turbine with those obtained for reference axial-flow turbines. Two such turbines are described in references 4 and 5 where the efficiency was constant beyond a certain Reynolds number level (ref. 5) or was essentially independent of Reynolds number over the range covered (ref. 4, turbine without downstream stator).

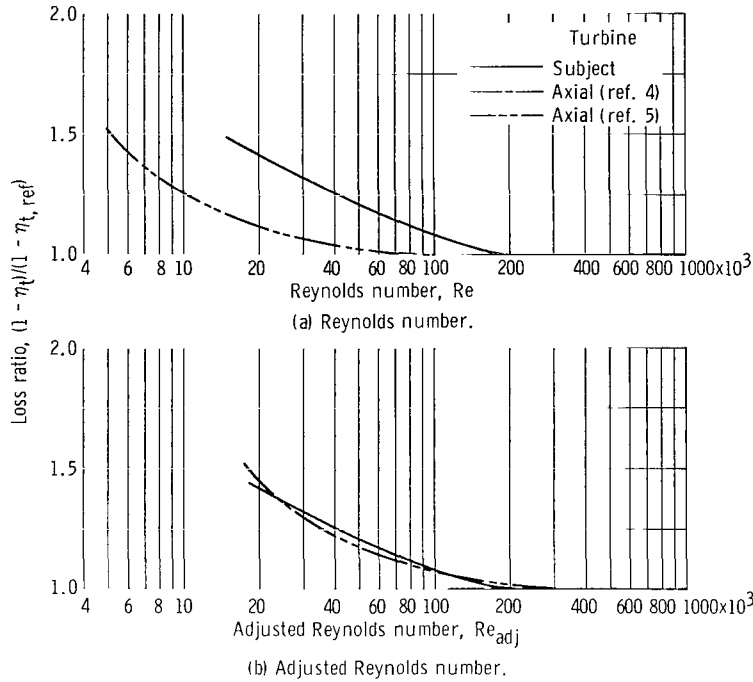


Figure 11. - Comparison of loss ratio as function of Reynolds number at design equivalent speed and pressure ratio.

Figure 11(a) presents a loss ratio $(1 - \eta_t)/(1 - \eta_{t, \text{ref}})$ as a function of Reynolds number as defined herein for the subject and reference turbines. The value of $1 - \eta_{t, \text{ref}}$ was determined from the maximum efficiency obtained. A good correlation is not obtained, which indicates that certain factors required for such a correlation were not included.

There are many factors that could affect the correlation of loss with Reynolds number. One effect might be the turbine reaction, which was substantially different for the turbines studied. For example, whereas the subject turbine had high reaction throughout, the turbine of reference 5 had a slight negative reaction across the rotor. Another consideration, however, is that of the definition of Reynolds number as used for the correlation. This definition, $w/\mu r$, was obtained from the fundamental relation $\rho Vc/\mu$ under the assumption that the geometry of the turbine would not differ greatly. (See refs. 2 and 11.) Among these geometric parameters was the blading aspect ratio \mathcal{A} which, in general, varies within reasonably close limits. However, for the axial turbines being compared herein, the aspect ratios differ considerably, with that of reference 5 being exceptionally low. Accordingly, inclusion of the aspect-ratio variation might improve the loss correlation.

Examination of the Reynolds number equations indicates that if aspect ratio is considered as a variable the expression would involve this parameter as $(w/\mu r)(1/\mathcal{A})$.

Therefore, the Reynolds numbers of the two reference turbines were adjusted to compensate for the differences in aspect ratio by using the following relation:

$$Re_{adj} = Re_{reference\ turbine} \frac{A_{subject\ turbine}}{A_{reference\ turbine}}$$

For this calculation, the value of aspect ratio used was the average of those for the stator and rotor. Figure 11(b) presents the loss ratio for the three turbines as a function of the adjusted Reynolds number. Here it is shown that the curves, and in particular that of the reference 5 turbine, shift over to a point where a reasonably good correlation is obtained.

The results just described must, to some extent, be considered qualitative since the level of Reynolds number for maximum efficiency for two of the turbines was not determined and since the value of maximum efficiency for the subject turbine was not established. The comparisons were made principally to indicate the need for proper consideration of the Reynolds number definition when attempting a correlation where various turbine designs are considered.

SUMMARY OF RESULTS

The effect of Reynolds number on the performance of an 8.5-inch- (21.59-cm-) mean-diameter, two-stage, axial-flow turbine is presented. The turbine was investigated in argon over a range of inlet pressures from about 1.0 to 9.0 psia (0.68 to 6.2 N/cm² abs) at design equivalent speed and various pressure ratios. At design equivalent pressure ratio, this range of inlet pressures corresponds to a range of Reynolds number from 18 000 to 177 000. The results of this investigation are presented, and the aerodynamic losses are compared with those measured for several other turbines. The results of the investigation are summarized as follows:

1. At design equivalent speed and pressure ratio, there was a 5.8 percent increase in mass flow over the range of Reynolds number covered. This variation occurred because of the decreased stator viscous losses and in a manner similar to that predicted from reference fluid meter data.

2. The total efficiency at design equivalent speed and pressure ratio increased from 0.82 to 0.88 over this same Reynolds number range. The corresponding static efficiency increased from 0.80 to 0.86. This increase in efficiency was attributed to the associated decrease in viscous losses since the rotor reaction was independent of Reynolds number.

3. The variation in loss with change in Reynolds number agreed well with a theoretical variation wherein 0.7 of the loss was attributed to viscous losses and the remaining 0.3 was attributed to other losses which are independent of Reynolds number. This variation is similar to that for two reference radial turbines investigated over a comparable range of Reynolds number.

Lewis Research Center,
National Aeronautics and Space Administration,
Cleveland, Ohio, October 10, 1967,
120-27-03-13-22.

APPENDIX - SYMBOLS

A	flow area, in. ² (cm ²)
\mathcal{A}	aspect ratio, h/c
c	chord length, ft (m)
g	gravitational constant, 32.174 ft/sec ²
h	blade height, ft (m)
Δh	specific work, Btu/lb (J/g)
J	mechanical equivalent of heat, 778.029 ft-lb/Btu
N	turbine speed, rpm
p	pressure, psia (N/cm ² abs)
Re	Reynolds number, $w/\mu r_m$
r_m	mean radius, ft (m)
T	absolute temperature, °R (°K)
U	blade velocity, ft/sec (m/sec)
V	absolute gas velocity, ft/sec (m/sec)
V_j	ideal jet speed corresponding to total- to static-pressure ratio across turbine, $\sqrt{2gJ \Delta h_{id}}$, ft/sec (m/sec)
W	relative gas velocity, ft/sec (m/sec)
w	mass flow, lb/sec (kg/sec)
α	absolute gas flow angle measured from axial direction, deg
γ	ratio of specific heats
δ	ratio of inlet total pressure to U.S. standard sea-level pressure, p'_1/p^*
ϵ	function of γ used in relating parameters to those using air inlet conditions at U.S. standard sea-level conditions, $\gamma^*/\gamma \left\{ \left[(\gamma+1)/2 \right]^{\gamma/(\gamma-1)} / \left[(\gamma^*+1)/2 \right]^{\gamma^*/(\gamma^*-1)} \right\}$
η_s	static efficiency (based on inlet-total- to exit-static-pressure ratio)
η_t	total efficiency (based on inlet-total- to exit-total-pressure ratio)
θ_{cr}	squared ratio of critical velocity at turbine-inlet temperature to critical velocity at U.S. standard sea-level temperature, $(V_{cr}/V_{cr}^*)^2$

μ gas viscosity, lb/(ft)(sec) (kg/(m)(sec))

ν blade-jet speed ratio, U_m/V_j

ρ gas density, lb/ft³ (kg/m³)

τ torque, in. -lb (N-m)

Subscripts:

adj adjusted

cr condition corresponding to Mach 1

eq air equivalent (U. S. standard sea level)

id ideal

ref reference

1 station at turbine inlet

2 station at first-stage stator exit

3 station at first-stage rotor exit

4 station at second-stage stator exit

5 station at second-stage rotor exit

Superscripts:

' absolute total state

* U. S. standard sea-level conditions (temperature, 518.67⁰ R (288.15⁰ K); pressure, 14.70 psia (10.13 N/cm²))

REFERENCES

1. Bernatowicz, Daniel T.: NASA Solar Brayton Cycle Studies. Paper presented at the Symposium on Solar Dynamics Systems. Solar and Mechanics Working Groups of the Interagency Advanced Power Group, Washington, D. C., Sept. 24-25, 1963.
2. Holeski, Donald E.; and Futral, Samuel M., Jr.: Experimental Performance Evaluation of a 6.02-Inch Radial-Inflow Turbine Over a Range of Reynolds Number. NASA TN D-3824, 1967.
3. Nusbaum, William J.; and Wasserbauer, Charles A.: Experimental Performance Evaluation of a 4.59-Inch Radial-Inflow Turbine Over a Range of Reynolds Number. NASA TN D-3835, 1967.
4. Forrette, Robert E.; Holeski, Donald E.; and Plohr, Henry W.: Investigation of the Effects of Low Reynolds Number Operation on the Performance of a Single-Stage Turbine with a Downstream Stator. NASA TM X-9, 1959.
5. Klassen, Hugh A.; and Wong, Robert Y.: Performance in Air of 4-Inch- (10.16-cm-) Mean-Diameter Single-Stage Axial Flow Turbine for Reynolds Numbers From 4900 to 188 000. NASA TN D- , 1968.
6. Wong, Robert Y.; and Nusbaum, William J.: Air-Performance Evaluation of a 4.0-Inch-Mean-Diameter Single-Stage Turbine at Various Inlet Pressures From 0.14 to 1.88 Atmospheres and Corresponding Reynolds Numbers from 2500 to 50,000. NASA TN D-1315, 1962.
7. Kofskey, Milton G.; and Glassman, Arthur J.: Turbomachinery Characteristics of Brayton-Cycle Space Power-Generation Systems. Paper No. 64-GTP-23, ASME, Mar. 1964.
8. Kofskey, Milton G.; and Nusbaum, William J.: Aerodynamic Evaluation of Two-Stage Axial-Flow Turbine Designed for Brayton Cycle Space Power System. NASA TN D- , 1968.
9. ASME Research Committee on Fluid Meters: Fluid Meters: Their Theory and Application. Fifth ed., ASME, 1959.
10. Shepherd, D. G.: Principles of Turbomachinery. The MacMillan Co., 1956.
11. Miser, James W.; Stewart, Warner L.; and Whitney, Warren J.: Analysis of Turbomachine Viscous Losses Affected by Changes in Blade Geometry. NACA RM E56F21, 1956.

11U 001 28 51 3DS 68059 00903
AIR FORCE WEAPONS LABORATORY/AFWL/
KIRTLAND AIR FORCE BASE, NEW MEXICO 87117

ATTN MISS MADELINE F. CANOVA, CHIEF TECHNIC
LIBRARY /WLIL/

POSTMASTER: If Undeliverable (Section 158
Postal Manual) Do Not Return

"The aeronautical and space activities of the United States shall be conducted so as to contribute . . . to the expansion of human knowledge of phenomena in the atmosphere and space. The Administration shall provide for the widest practicable and appropriate dissemination of information concerning its activities and the results thereof."

—NATIONAL AERONAUTICS AND SPACE ACT OF 1958

NASA SCIENTIFIC AND TECHNICAL PUBLICATIONS

TECHNICAL REPORTS: Scientific and technical information considered important, complete, and a lasting contribution to existing knowledge.

TECHNICAL NOTES: Information less broad in scope but nevertheless of importance as a contribution to existing knowledge.

TECHNICAL MEMORANDUMS: Information receiving limited distribution because of preliminary data, security classification, or other reasons.

CONTRACTOR REPORTS: Scientific and technical information generated under a NASA contract or grant and considered an important contribution to existing knowledge.

TECHNICAL TRANSLATIONS: Information published in a foreign language considered to merit NASA distribution in English.

SPECIAL PUBLICATIONS: Information derived from or of value to NASA activities. Publications include conference proceedings, monographs, data compilations, handbooks, sourcebooks, and special bibliographies.

TECHNOLOGY UTILIZATION PUBLICATIONS: Information on technology used by NASA that may be of particular interest in commercial and other non-aerospace applications. Publications include Tech Briefs, Technology Utilization Reports and Notes, and Technology Surveys.

Details on the availability of these publications may be obtained from:

SCIENTIFIC AND TECHNICAL INFORMATION DIVISION
NATIONAL AERONAUTICS AND SPACE ADMINISTRATION

Washington, D.C. 20546